ARMY RESEARCH LABORATORY

Actuator Characterization of Man Portable Precision Maneuver Concepts

by Frank Fresconi, Ilmars Celmins, and Bryant Nelson

ARL-TR-6841 **March 2014**

NOTICES

Disclaimers

The findings in this report are not to be construed as an official Department of the Army position unless so designated by other authorized documents.

Citation of manufacturer's or trade names does not constitute an official endorsement or approval of the use thereof.

Destroy this report when it is no longer needed. Do not return it to the originator.

Army Research Laboratory
Aberdeen Proving Ground, MD 21005-5069

ARL-TR-6841 **March 2014**

Actuator Characterization of Man Portable Precision Maneuver Concepts

Frank Fresconi and Ilmars Celmins
Weapons and Materials Research Directorate, ARL

Bryant Nelson
Bowhead Science and Technology
Belcamp, MD 21017

REPORT DOCUMENTATION PAGE	Form Approved OMB No. 0704-0188

1. REPORT DATE *(DD-MM-YYYY)*	2. REPORT TYPE	3. DATES COVERED (From - To)
March 2014	Final	October 2012–September 2013

4. TITLE AND SUBTITLE
Actuator Characterization of Man Portable Precision Maneuver Concepts

5a. CONTRACT NUMBER

5b. GRANT NUMBER

5c. PROGRAM ELEMENT NUMBER

6. AUTHOR(S)
Frank Fresconi, Ilmars Celmins, and Bryant Nelson

5d. PROJECT NUMBER
AH43

5e. TASK NUMBER

5f. WORK UNIT NUMBER

7. PERFORMING ORGANIZATION NAME(S) AND ADDRESS(ES)
U.S. Army Research Laboratory
ATTN: RDRL-WML-E
Aberdeen Proving Ground, MD 21005-5066

8. PERFORMING ORGANIZATION REPORT NUMBER
ARL-TR-6841

9. SPONSORING/MONITORING AGENCY NAME(S) AND ADDRESS(ES)

10. SPONSOR/MONITOR'S ACRONYM(S)

11. SPONSOR/MONITOR'S REPORT NUMBER(S)

12. DISTRIBUTION/AVAILABILITY STATEMENT
Approved for public release; distribution is unlimited.

13. SUPPLEMENTARY NOTES

14. ABSTRACT
This report examines maneuvering a man-portable precision projectile. A class of innovative maneuver concepts that relies on rotational actuation for small diameter, high spin rate, gun-launched projectiles is proposed. The performance of the actuation technology associated with this class of maneuver concepts is addressed. Actuator experiments conducted over a variety of conditions validate dynamic models of the actuator and supply the data necessary for model parameter estimation. Actuator performance metrics of spin rate response, friction, and power requirements were derived from the data. This study indicates that this class of maneuver concepts can be driven with these actuators. These results enable actuator design and multidisciplinary simulation of refined maneuver concepts for a specific application.

15. SUBJECT TERMS
Maneuver, projectile, actuation technology, spin-stabilization, parameter estimation

16. SECURITY CLASSIFICATION OF:			17. LIMITATION OF ABSTRACT	18. NUMBER OF PAGES	19a. NAME OF RESPONSIBLE PERSON
a. REPORT	b. ABSTRACT	c. THIS PAGE			Frank Fresconi
Unclassified	Unclassified	Unclassified	UU	26	19b. TELEPHONE NUMBER (*Include area code*) 410-306-0794

Contents

List of Figures iv

List of Tables iv

1. Introduction 1

2. Concepts 2

3. Actuator Characterization 4

3.1 Experimental Setup 4

3.2 Raw Experimental Data....6

3.3 Experimental Uncertainty....8

3.4 Conversion to Engineering Units 9

3.5 Data Modeling....10

3.6 Physical Modeling....10

3.7 Parameter Estimation 11

4. Results and Discussion 12

5. Conclusions and Future Work 16

6. References 17

Distribution List 19

List of Figures

Figure 1. Rotating wing maneuver concept. 2
Figure 2. Snapshots (viewed from base in an Earth-fixed reference frame) over one revolution of rotating wing maneuver concept with two actuators. 3
Figure 3. Rotating finned base maneuver concept. 4
Figure 4. Image of motor with rotating wing concept and prototype 40-mm projectile. 5
Figure 5. Schematic of experimental setup. 6
Figure 6. Image of experimental setup. 6
Figure 7. Raw input signal. 7
Figure 8. Raw output signal. 8
Figure 9. Manipulated input signal. 9
Figure 10. Manipulated output signal. 10
Figure 11. Measured and calculated spin rate. 13
Figure 12. Current history. 14

List of Tables

Table 1. Motor electrical and inertial data. 5
Table 2. Individual experiment maneuver system parameters. 15
Table 3. Summary statistics of the maneuver system parameters. 15

1. Introduction

The motivation for this report is to maneuver man-portable precision munitions. In-flight airframe maneuvers are required to overcome uncompensated ballistic error sources such as launch variation and atmospheric disturbances or engage targets in defilade, to ultimately improve lethality. Man-portable precision capability provides enhanced lethality at the squad level.

Various methods have been devised to course-correct the flight of projectiles (*1*–*11*). Aerodynamic (*1, 3, 4, 6*–*11*) or mass (*5*) asymmetries are often used. Lateral jet thrusters are another means (*2, 7*). Providing maneuver technologies in the man-portable, gun-launched environment is extremely challenging. The loads imparted to electro-mechanical components during the gun launch event are high (*12, 13*). Size, weight, power, and cost needs are difficult to meet. Man-portable weapons are about 80 mm in diameter or smaller. Maneuver systems, which usually include a power source, actuators, sensors, processors, and associated electronics, must fit along with other sub-systems in this small package. The cost of these technologies must be low to ensure high volume proliferation to individual Soldiers on the battlefield. Depending on caliber, the dynamic pressure available for aerodynamic control authority (essentially, the projectile velocity) may be limited due to gun recoil limits on the human shoulder. Lastly, rifled guns often induce high spin rates (hundreds or thousands of cycles per second) in the projectile, which can significantly stress the bandwidth requirements of maneuver technologies. This study proposes a class of maneuver concepts, based on rotational actuation, to overcome these challenges in the man-portable precision problem

Comprehensive investigation of a projectile maneuver concept implies consideration of aeromechanics, flight control, structural dynamics, and actuation technology. Actuators, the focus of this study, underpin the maneuver concept and are essential to guided flight. Actuator performance requirements are met through a fundamental understanding of actuator behavior. The response of actuators can be described with theoretical models, which are driven with empirically derived data. Electric motors are commonly applied in rotational actuation schemes and often model response by considering the applied torques (e.g., motor, friction) in Newton's 2nd law. Experiments conducted on actuation system assemblies (e.g., motor, linkages, aerodynamic surfaces) can be combined with theoretical models to obtain critical actuation technology parameters.

This study focuses on characterizing actuation technologies specific to the proposed class of maneuver concepts. Actuator experiments are conducted to identify theoretical models and estimate parameters of these models. Actuator performance metrics for the present application include torque, response, friction, and power requirements. Characterization of the actuation technology permits feasibility assessment, simulation of guided flight performance, and design

for guided projectile demonstration. This study provides a somewhat general actuator characterization to cover a wider application space. Specific applications dictate performance requirements for more detailed actuator design.

This report is organized as follows: maneuver concepts are first outlined, followed by a discussion of actuator experiments to include the setup, raw and manipulated data, experimental uncertainty, theoretical modeling, and parameter estimation algorithm, and then results are presented prior to summarizing the report with conclusions and future work.

2. Concepts

While the intent is to research maneuver technology with a wide applicability, a few general constraints may be imposed. The application under investigation is a spin-stabilized projectile. Spin rates are in the range of 50–300 Hz. For the purposes of preliminary design, a 40-mm projectile was used.

Given this information, some concepts were formulated around a central theme. The common element is a rotational actuator. The idea is that small linear actuators may not be able to move aerodynamic surfaces at rates of 50–300 Hz with high precision at low cost, but rotational actuators may. This is because a linear (reciprocating) actuator would need to constantly change direction, resulting in large accelerations, which, in turn, require large forces, thereby driving up the actuator power. A rotational actuator would be operating at a fairly constant rotation once it is up to speed, resulting in much lower power requirements.

Figure 1 illustrates a concept using one or more wings fixed to a rotational actuator. As the projectile spins, the actuator rotates at the same rate in the opposite direction. Over one spin cycle, the wing rotates from stowed internally within the projectile body to fully exposed to the airstream to effect lateral maneuver (as shown in the rendering of figure 1) to again stowed within the projectile. Shifting the phase of the rotational actuator with respect to the projectile spin enables maneuvering in any direction.

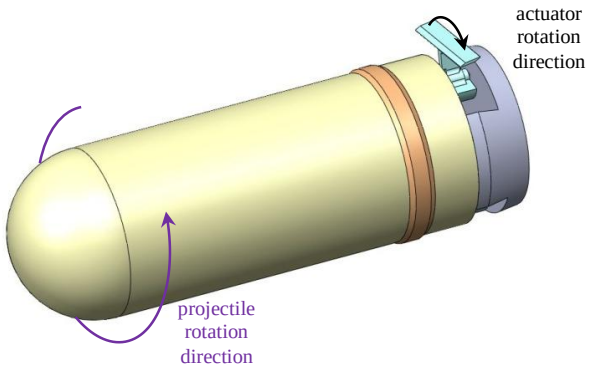

Figure 1. Rotating wing maneuver concept.

Figure 2 depicts the manner in which a two-actuator variant of this concept operates over a complete cycle of spin. The maneuver concept is viewed from the base of the projectile at eight snapshots (corresponding to a change in roll angle of 45°) throughout the spin cycle. Successive snapshots of the concept throughout the spin cycle proceed in a counterclockwise manner around the figure. When viewed from the base the projectile spins in the clockwise direction and the actuator assembly rotates in a counterclockwise direction. In this manner, the wings attached to each actuator rotate in and out of the projectile to provide a consistent maneuver direction.

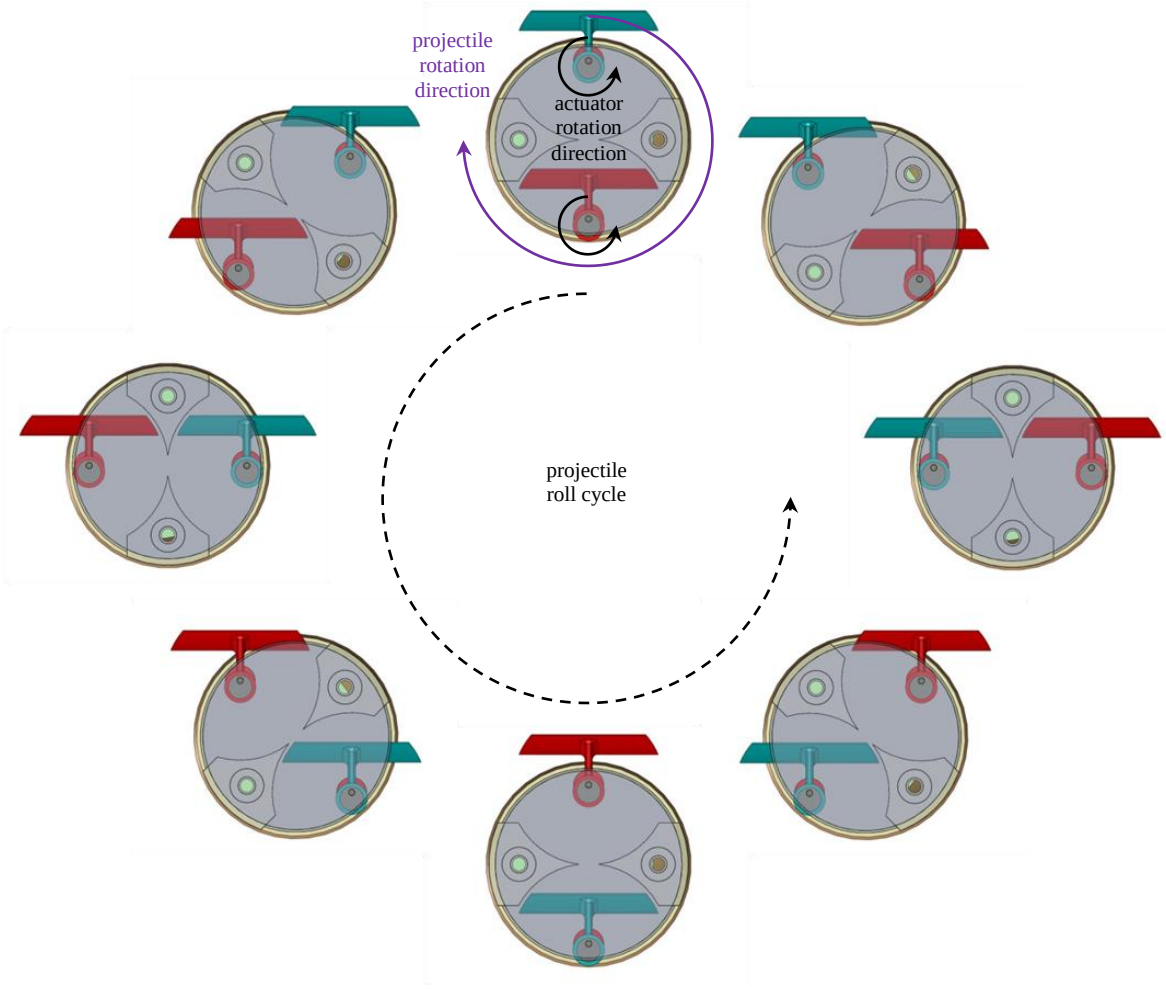

Figure 2. Snapshots (viewed from base in an Earth-fixed reference frame) over one revolution of rotating wing maneuver concept with two actuators.

Another concept with this rotational actuator theme is presented in figure 3. Here, a single rotational actuator is mounted to a projectile base assembly featuring a pair of deflected fins, which deploy after launch. The actuator rotates the finned base opposite the projectile spin so that the aerodynamic asymmetry of the deflected fins produces a lateral maneuver. Again, phase shifting the finned base rotation with respect to the projectile rotation yields maneuvers in any direction.

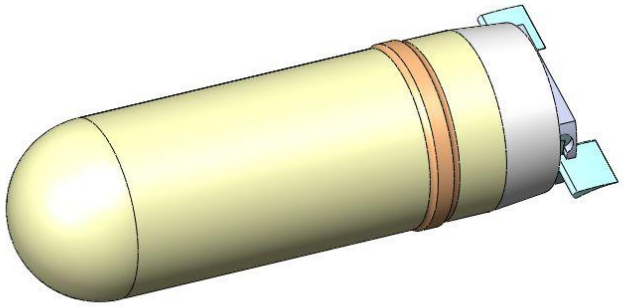

Figure 3. Rotating finned base maneuver concept.

These maneuver concepts are on the rear of the projectile to facilitate packaging within the mouth of the cartridge case to reduce the handling and storage burden. The specific configuration of the maneuver system and aerodynamic surfaces to achieve control authority requirements for these concepts depends on the mission (e.g., launch and flight conditions, system errors, etc.)

3. Actuator Characterization

Experiments were conducted to characterize the actuation technology for this class of maneuver concepts. Small, low-cost, gun-hard motors were obtained and assembled into prototype maneuver systems. Theoretical actuator dynamics were identified by collecting data on the input (motor) and output (spin rate) of the system. Experimental parameters included motor size, commanded spin rate, rotational direction, and inertial load. This analysis quantified key performance metrics such as response, friction, and power requirements, which can be used in maneuver concept refinement for a particular application.

3.1 Experimental Setup

An apparatus was created for data collection. A market survey yielded some viable motors (manufactured by Maxon). An image of one of these brushless DC motors, along with a model of the rotating wing concept and a prototype 40-mm projectile, which was fired through the spark range (*14*), is shown in figure 4. This motor product line goes down to 6 mm in diameter with

satisfactory cost, speed and torque specifications. Electrical (e.g., torque constant K_T) and inertial (moment of inertia I_X, diameter D) data for some of these motors are given in table 1. Shock table experiments also indicated favorable survivability characteristics.

Figure 4. Image of motor with rotating wing concept and prototype 40-mm projectile.

Table 1. Motor electrical and inertial data.

Part No.	**Voltage (V)**	K_T **(Nm/A)**	I_X **(kg-m^2)**	D **(m)**
250101	12	2.9×10^{-3}	5×10^{-10}	0.006
283828	12	8.23×10^{-3}	4.28×10^{-8}	0.016

An experimental setup was created in the laboratory to operate these motors unloaded and with various control mechanism (inertial and aerodynamic) loadings at different speeds. Figure 5 provides a schematic of the setup. A speed controller (E-flite 10-A Pro Brushless Electronic Speed Controller) was used to drive the three motor commutator input lines. This controller inputs a pulse-width modulated (PWM) signal from a signal generator proportional to the desired spin rate and used the voltage generated by the spinning motor to infer the spin rate (back electromotive force) for feedback control purposes. The motor was equipped with 3 Hall effect sensors for measuring response. A data acquisition board (National Instruments USB-6259) run by LabView software was used to collect the input PWM and motor signals and output Hall sensor data. An image of this setup on the bench in the laboratory is shown in figure 6.

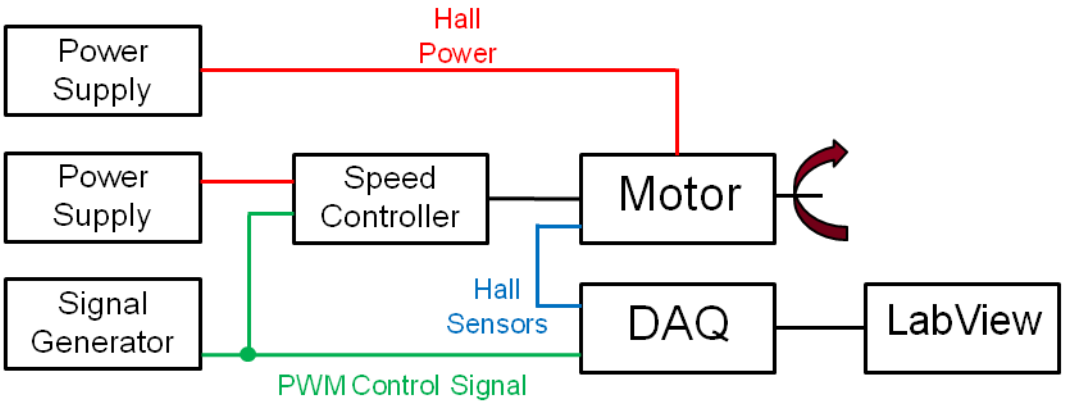

Figure 5. Schematic of experimental setup.

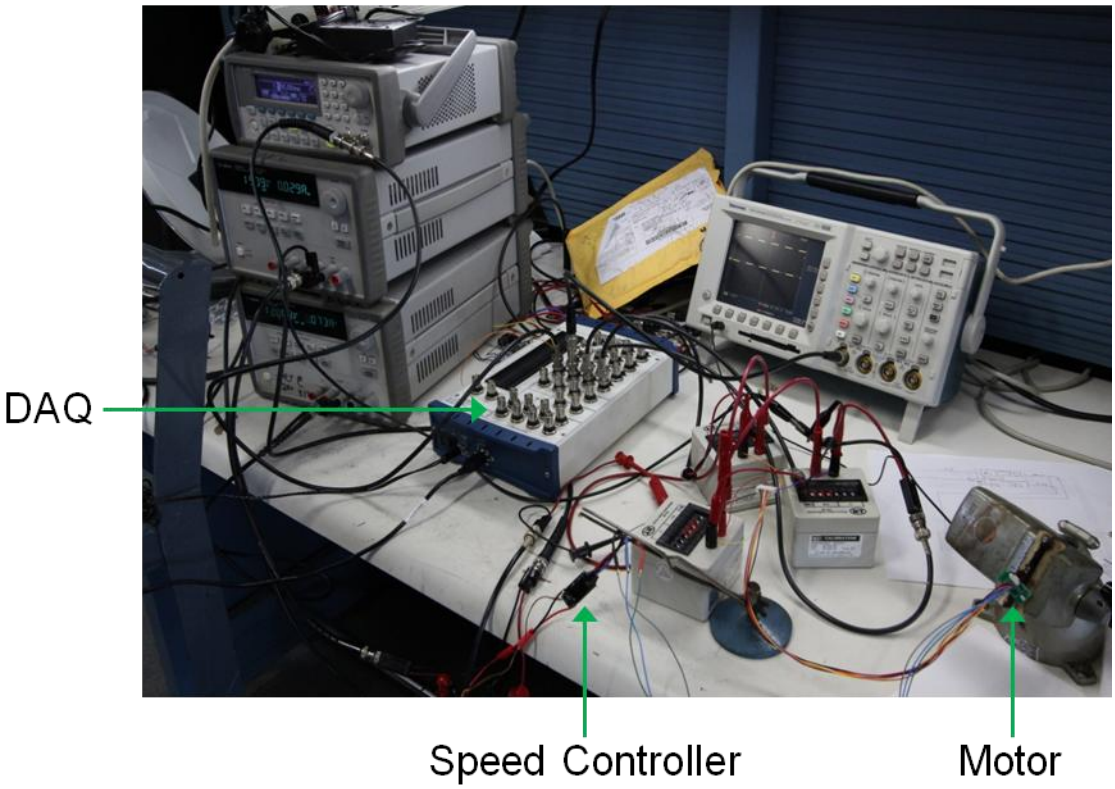

Figure 6. Image of experimental setup.

3.2 Raw Experimental Data

Collection of actuation system input and output is necessary to derive theoretical models and estimate model parameters. An example of the raw input data scaled to about 10 V in the data acquisition from an experiment is provided in figure 7. The motor driving signal leading and trailing edge times were interrogated to within a half-sample time resolution for determining the pulse width. The motor spin rate was controlled using the pulse width of the input signal rather than the amplitude of the input signal.

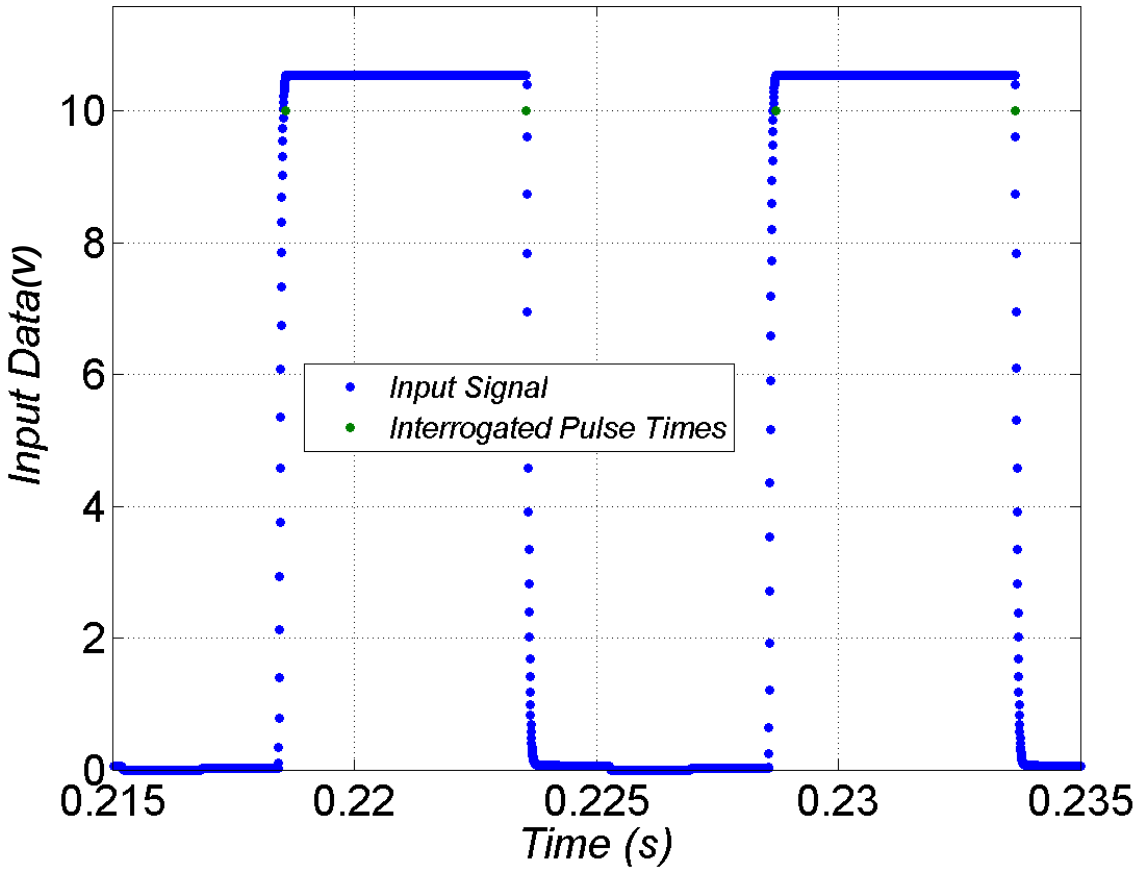

Figure 7. Raw input signal.

A sample of the output of one of the channels of Hall sensor data is shown in figure 8. A cycle of low (0 V) and high (5 V) signal represents one rotation. Interrogation of the Hall pulse leading and trailing edges over one rotation permits calculation of the spin rate. The sample data in figure 8 correspond to a spin rate of about 35.7 Hz.

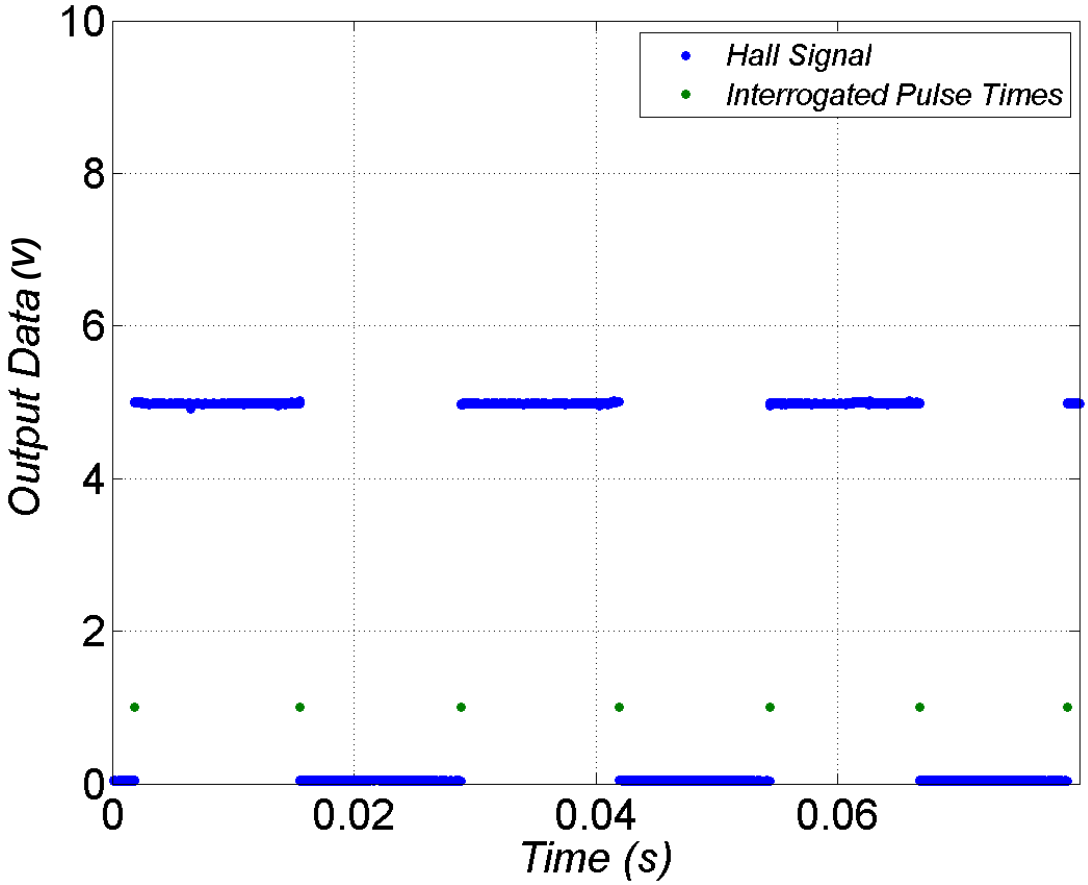

Figure 8. Raw output signal.

3.3 Experimental Uncertainty

Consideration of the experimental uncertainty in spin rate is merited, especially since only Hall sensor pulses (i.e., not a high resolution encoder) are used. A simple equation relates the primary experimental measurement (time to complete one rotation Δt) to the spin rate ($\dot{\phi}$) in Hz.

$$\dot{\phi} = \frac{1}{\Delta t} \tag{1}$$

The relationship between the uncertainty in the spin rate measurement ($w_{\dot{\phi}}$) to the uncertainty in the primary measurement ($w_{\Delta t}$) is given.

$$w_{\dot{\phi}} = \sqrt{\left(\frac{\partial \dot{\phi}}{\partial \Delta t} w_{\Delta t}\right)^2} = \frac{1}{\Delta t^2} \frac{1}{2 f_s} \tag{2}$$

This expression highlights the importance of a high data sample rate (f_s). Uncertainty in spin rate on the order of 0.1 Hz may be expected at a 10-kHz sample rate for a 50-Hz spin rate. A sample rate of 200 kHz was used in the experiments ($w_{\dot{\phi}} \sim 0.001$Hz).

3.4 Conversion to Engineering Units

The motor driving signals were used to obtain the system input data shown in figure 9. The pulse width for all three signals to the motor and an average are provided. In this experiment, the controller calls for higher demand when spinning the control mechanism up followed by a lower control effort once the assembly reaches a steady-state spin rate.

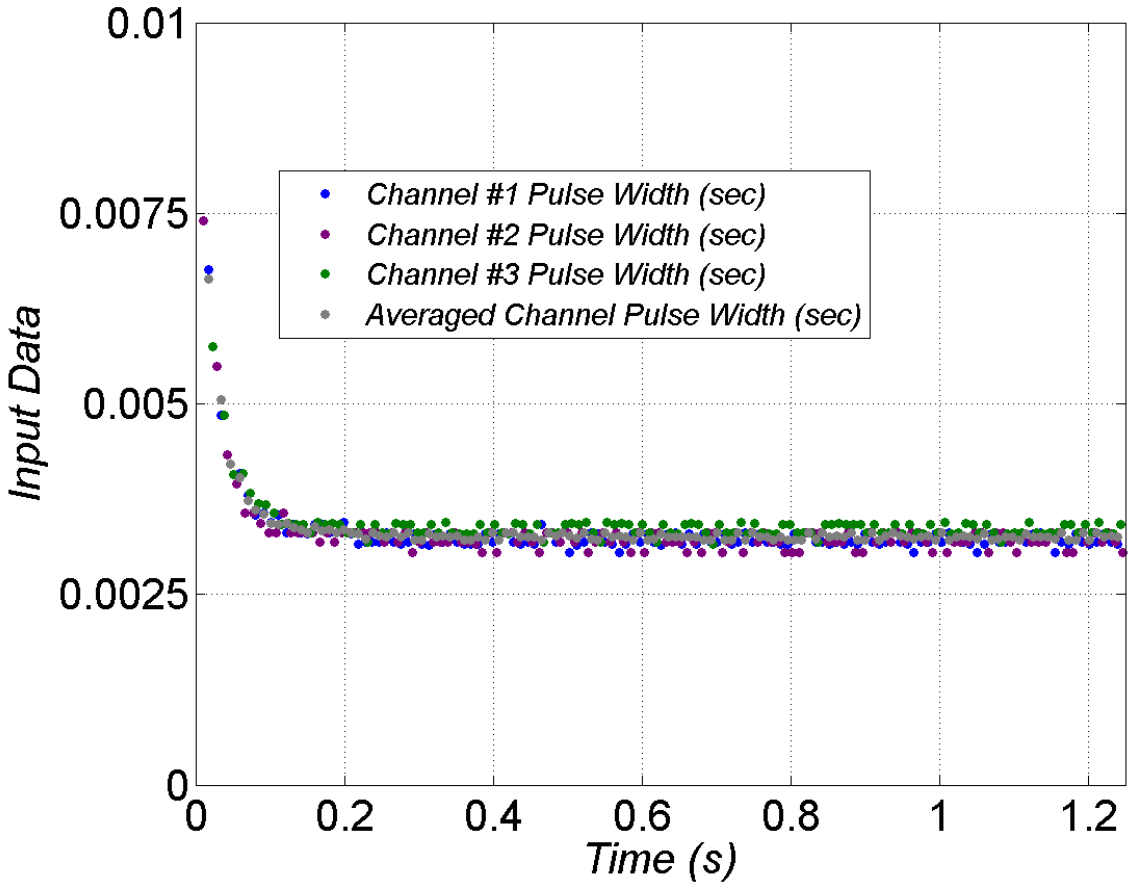

Figure 9. Manipulated input signal.

The Hall sensor output was manipulated to determine spin rate. Additionally, an average spin rate was found by averaging the spin rate and time of individual Hall sensors. An example of these data is provided in figure 10. The actuator reaches a spin rate of over 100 Hz within about 0.1 s. Fluctuation in the steady-state spin rate may be due to controller performance at this low load. One Hall sensor was not recorded during this experiment.

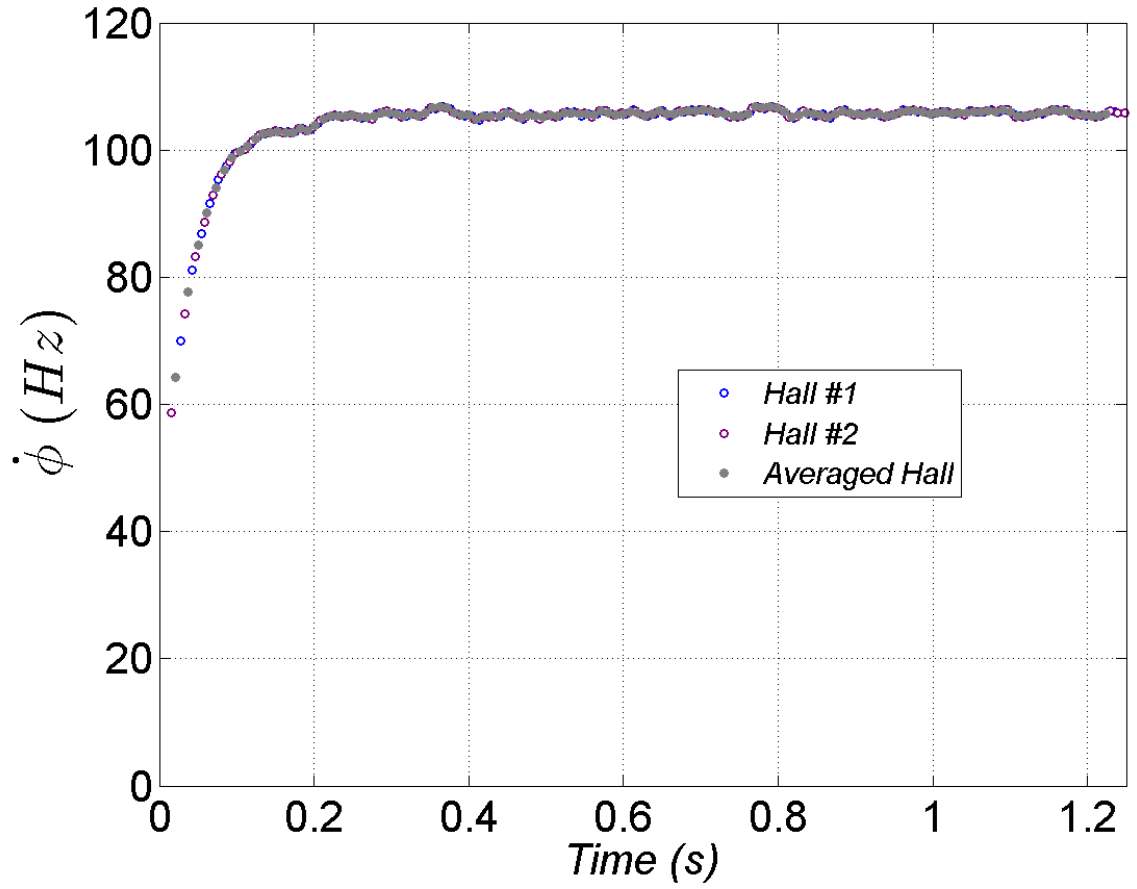

Figure 10. Manipulated output signal.

3.5 Data Modeling

Inspection of the spin rate response in figure 10 suggests a simple model may capture the experimental data. A first order system was used to model the data in preliminary experiments. A lag, dictated by the time constant ($\tilde{\tau}$), prescribes the manner in which the spin rate adjusts to a commanded spin rate ($\dot{\phi}_c$).

$$\tilde{\tau}\ddot{\phi} + \dot{\phi} = \dot{\phi}_c \tag{3}$$

Pulse width (P), rather than commanded spin rate, is the driving input in experiments due to the manner in which the experiments were conducted ($\dot{\phi}_c = f_p P$). These inputs relate through a scaling (f_p).

3.6 Physical Modeling

Newtonian kinetics is applied about the spin axis of the maneuver system to derive the dynamic equation of motion from first principles. The dynamics are driven by the total axial moment of inertia, friction moment (friction coefficient K_F), and the driving moment (torque constant K_T and average current $\bar{\imath}$ (*15–17*).

$$I_X\ddot{\phi} = K_F\dot{\phi} + K_T\bar{\imath} \tag{4}$$

Inspection of the equivalent models in equations 3 and 4 permits relationships between model parameters to be defined.

$$K_F = \frac{I_X}{\tilde{\tau}} \tag{5}$$

$$\bar{\imath} = \frac{f_p P K_F}{K_T} \tag{6}$$

The time constant in the data model does not adhere to the classic definition of time constant. A more traditional time constant may by derived from model parameters ($\tau = \frac{\tilde{\tau} I_X}{K_F}$).

3.7 Parameter Estimation

Parameters in the physical models must be characterized for actuator performance evaluation and for multidisciplinary modeling and simulation of other aspects (maneuver system control, aeromechanics, flight control) of a man-portable precision munition. A variety of parameter estimation routines may be formulated for the current problem. The maximum likelihood method (*18–22*) was chosen based on the ease of use and attractiveness for this application. In this scheme, a likelihood function is defined.

$$\mathcal{L} = \frac{1}{(2\pi)^{\frac{N_M}{2}}\sqrt{\vec{R}}} exp\left(-\frac{1}{2}\vec{e}^T\vec{R}^{-1}\vec{e}\right) \tag{7}$$

Here, the residual ($\vec{e} = \vec{x}_M - \vec{x}_C$) is the difference between measurements and theoretical model calculations and the residual covariance ($\vec{R} = E[\vec{e}\vec{e}^T]$) for the current problem represents experimental uncertainty. The number of measurements are N_M. The goal of this parameter identification algorithm is to find the model parameters that optimize the likelihood function (and thereby minimize the difference between measurements and model calculations).

If model noise is neglected, then some simplifications to the general maximum likelihood method can be made. The algorithm starts by inputting estimates of the initial states, parameters, and measurement uncertainty. The model is integrated with states ($\vec{x}_C$), controls ($\vec{u}$), and parameters ($\vec{\theta}^j$).

$$\dot{\vec{x}}_C = f\left(\vec{x}_C, \vec{u}; \vec{\theta}^j\right) \tag{8}$$

This method accommodates nonlinear models. For the current problem, the equation of motion in equation 3 was used as the model with $\vec{x}_C = \dot{\phi}$, $\vec{u} = P$, and $\vec{\theta} = [\tilde{\tau} \quad f_p]^T$.

At times when measurements are available, a Newton-Raphson method optimizes the likelihood function. Calculations are performed for the residual and Jacobian ($\frac{\partial \vec{x}_C}{\partial \vec{\theta}}$).

$$\frac{\partial \vec{x}_C}{\partial \vec{\theta}} = \begin{bmatrix} \frac{\partial x_{C_1}}{\partial \theta_1} & \frac{\partial x_{C_2}}{\partial \theta_2} & \cdots \\ \frac{\partial x_{C_2}}{\partial \theta_1} & \ddots & \vdots \\ \vdots & \cdots & \frac{\partial x_{C_{N_M}}}{\partial \theta_{N_P}} \end{bmatrix} \tag{9}$$

The number of parameters is N_P. The Jacobian may be found analytically or numerically. Forward differencing was used in the present problem.

Parameters are corrected through the following expression.

$$\Delta\vec{\theta} = \left(\sum_{i=1}^{N} \frac{\partial \vec{x}_{C,i}}{\partial \vec{\theta}}^T \vec{R}^{-1} \frac{\partial \vec{x}_{C,i}}{\partial \vec{\theta}} \right)^{-1} \sum_{i=1}^{N} \frac{\partial \vec{x}_{C,i}}{\partial \vec{\theta}}^T \vec{R}^{-1} \vec{e}_i \tag{10}$$

The number of measurement samples is N. The term $\sum_{i=1}^{N} \frac{\partial \vec{x}_{C,i}}{\partial \vec{\theta}}^T \vec{R}^{-1} \frac{\partial \vec{x}_{C,i}}{\partial \vec{\theta}}$ is often referred to as the information matrix and represents the content of useful data. The parameter estimation problem is ill-conditioned when the determinant of the information matrix is zero.

Corrections are applied to update the parameter estimates.

$$\vec{\theta}^{j+1} = \vec{\theta}^{j} + \Delta\vec{\theta} \tag{11}$$

The model is integrated again with the updated parameters.

$$\dot{\vec{x}}_C = f\left(\vec{x}_C, \vec{u}; \vec{\theta}^{j+1}\right) \tag{12}$$

The residual is recalculated. This process is iterated at each measurement update until some convergence criterion (e.g., magnitude of residual below some threshold) is reached. Once convergence is satisfied, the updated parameter estimates are used to integrate the model forward in time until the cycle repeats at the next measurement update. In this manner, calculated response and parameter estimates are obtained over the entire measurement history.

4. Results and Discussion

Actuator experiments were conducted over a variety of conditions and multiple samples at a given condition to assess full spectrum performance and perform statistical analysis. Independent parameters were motors (6 mm, 16 mm), commanded spin rate (approximately 50 Hz, 100 Hz), rotation direction (clockwise [CW], and counterclockwise [CCW]), and inertial load (motor only, added inertial). Data were collected for each case and analyzed as outlined above.

An example of the measured spin rate and spin rate calculated from the parameter estimation algorithm is provided in figure 11. The model matches the ramp-up and steady-state portions of the experimental data. Errors in spin rate were usually less than 1 Hz across experimental results. Agreement between the theory and experiment validates the models and data driving the models.

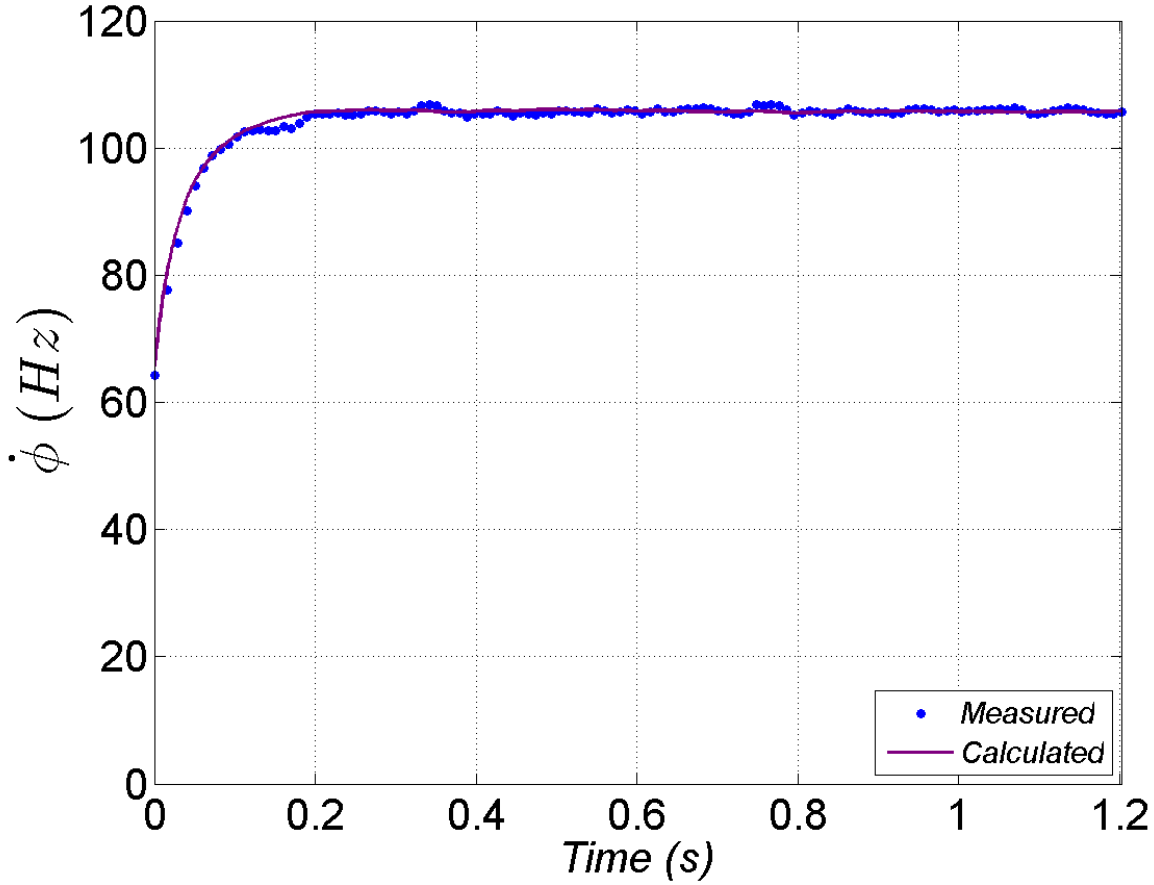

Figure 11. Measured and calculated spin rate.

The resulting parameter estimates and input data can be used to determine the current sent to the motor. Figure 12 shows that the current is higher when spinning the actuator up from rest before leveling off as the spin rate holds constant. All results indicate modest power requirements.

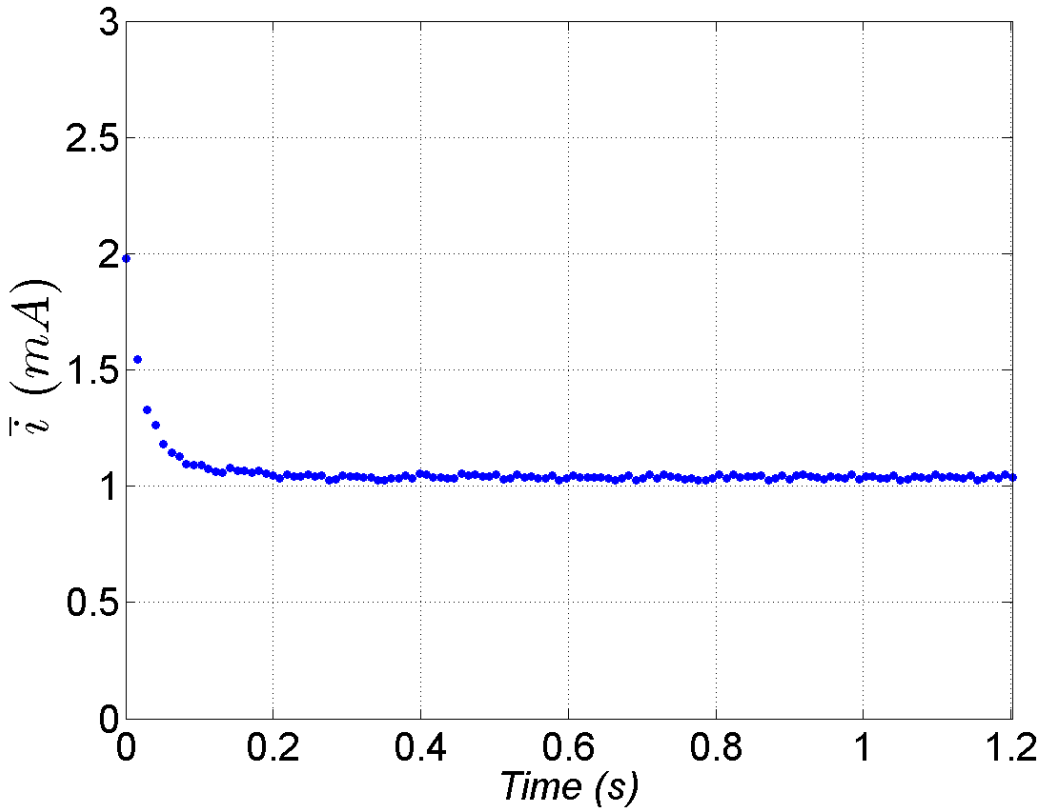

Figure 12. Current history.

Parameter estimates across the different experimental conditions are provided in table 2. All parameters are consistent for a given condition over multiple trials. The input scaling and average current varied with commanded spin rate and motor size as expected. The direction of rotation also changed the input scaling and average current mainly for the 6-mm-diameter motor at low commanded spin rate. When an additional inertia load was added to the assembly motor performance degraded. For this reason, few results with higher uncertainty are presented in table 2 for this situation.

Friction coefficient and time constant only varied according to the physical configuration. For this reason, statistics were calculated and are given in table 3. Inspection of these data demonstrates that the friction and time constant increases with motor size. The standard deviation of all parameters was within 10% of the mean.

Table 2. Individual experiment maneuver system parameters.

Motor Part No.	I_X (kg-m^2)	$\dot{\phi}_c$ (Hz)	dirn	$\tilde{\tau}$ (s)	f_p (rad/s/s)	K_F (Nm/rad/s)	τ (s)	$\bar{\imath}$ (mA)
250101	5.00E-10	50	CW	0.117799	59782.2	4.244523E-09	0.0138766	0.52077570
250101	5.00E-10	50	CW	0.119679	62197.4	4.177852E-09	0.0143230	0.52735538
250101	5.00E-10	50	CCW	0.119538	44430.4	4.182768E-09	0.0142893	0.45127208
250101	5.00E-10	50	CCW	0.120280	38149.5	4.156962E-09	0.0144673	0.41336654
250101	5.00E-10	100	CW	0.120413	135331.9	4.152359E-09	0.0144994	0.94948280
250101	5.00E-10	100	CW	0.119639	133474.5	4.179256E-09	0.0143134	0.95239048
250101	5.00E-10	100	CCW	0.109699	207084.4	4.557932E-09	0.0120338	1.06930253
250101	5.00E-10	100	CCW	0.109909	203795.0	4.549225E-09	0.0120799	1.06246883
250101	7.95E-08	100	CW	1.1001783	40312.1	7.226102E-08	1.2103922	9.4959481
250101	7.95E-08	100	CW	1.100049	20095.7	7.226950E-08	1.2101079	5.4555720
283828	4.28E-08	50	CW	0.210376	50336.7	2.034450E-07	0.0442582	0.00856922
283828	4.28E-08	50	CW	0.210347	51158.7	2.034733E-07	0.0442459	0.00841666
283828	4.28E-08	50	CCW	0.209893	55077.7	2.039136E-07	0.0440550	0.00869805
283828	4.28E-08	50	CCW	0.210176	54995.4	2.036385E-07	0.0441741	0.00868476
283828	4.28E-08	100	CW	0.211267	185285.5	2.025871E-07	0.0446338	0.01664861
283828	4.28E-08	100	CW	0.210160	186536.6	2.036542E-07	0.0441673	0.01612379
283828	4.28E-08	100	CCW	0.208431	187904.2	2.053441E-07	0.0434433	0.01649680
283828	4.28E-08	100	CCW	0.210147	188598.3	2.036670E-07	0.0441618	0.01636425

Table 3. Summary statistics of the maneuver system parameters.

Motor Part No.	I_X (kg-m^2)	N		$\tilde{\tau}$ (s)	K_F (Nm/rad/s)	τ (s)
250101	5.00E-10	8	μ	0.117119	4.275110E-09	0.0137354
			σ	0.004584	1.741363E-10	0.0010530
283828	4.28E-08	8	μ	0.210100	2.037154E-07	0.0441424
			σ	0.000787	7.661270E-10	0.0003304

Estimates of the friction coefficient are useful for predicting and manipulating the dynamic response of the maneuver system. The average current permits battery sizing. The input scaling allows precise spin rate setting for future experiments. Finally, the time constant provides a metric for the system response time. The average current, input scaling, and time constants are specific to the commercial speed controller used in the experiments.

This study provides general actuator performance indicators for a class of maneuver concepts. Overall, results indicate battery requirements and friction and spin rate characteristics of this actuation scheme are satisfactory for low loadings. The practical inertial (and potentially aerodynamic) loading, however, may demand an improved controller or motor with higher torque. Maneuver concept refinement for a particular application dictates the detailed actuator design.

5. Conclusions and Future Work

This report outlined actuator characterization of maneuver concepts for man-portable precision munitions. Multiple concepts, based on a common theme of aerodynamic control with a rotational actuator, were formulated. The specific details regarding practical implementation of these concepts for a particular mission must consider additional factors such as the control authority needed to deliver the lethal payload.

Experiments were conducted to assess actuator performance. This report provided the experimental setup along with the raw and manipulated data. Experimental uncertainty was considered. Data- and physics-based models of the actuation system were composed. A parameter estimation algorithm was introduced. Satisfactory matches between the experimental data and theory provided some verification of the actuator models as well as numeric values for the parameters. These models and data are essential to achieving actuation performance goals and multidisciplinary simulation of the man-portable precision munition.

Electro-mechanical design and analysis of actuator technologies in this report suggest feasibility with regard to cost, size, bandwidth, response, and power (even with a commercial controller). Overall, preliminary results indicated favorable characteristics of these maneuver concepts; however, further investigations must be performed. Dynamic behavior of the maneuver concept within a spinning body and under realistic aerodynamic loadings (e.g., in a wind tunnel) must be examined. The rotating wing and finned base concepts also need further refinement of electro-mechanical and control design. A careful survivability assessment must be made. The final task to enabling maneuvers for man-portable precision munitions is free-flight experimentation.

6. References

1. McMichael, J.; Lovas, A.; Plostins, P.; Sahu, J.; Brown, G.; Glezer, A. Microadaptive Flow Control Applied to a Spinning Projectile, AIAA-2004-2512.
2. Cooper, G.; Costello, M. Flight Dynamic Response of Spinning Projectiles to Lateral Impulsive Loads. *Journal of Dynamic Systems, Measurement, and Control* **2004**, *126*, 605–613.
3. Moorhead, J. S. Precision Guidance Kits (PGKs): Improving the Accuracy of Conventional Cannon Rounds. *Field Artillery* **January–February 2007**, 31–33.
4. Celmins, I. *Design and Evaluation of an Electromechanical Actuator for Projectile Guidance*; ARL- MR-0672; U.S. Army Research Laboratory: Aberdeen Proving Ground, MD, September 2007.
5. Rogers, J.; Costello, M.. Control Authority of a Projectile Equipped with a Controllable Internal Translating Mass. *Journal of Guidance, Control, and Dynamics* **2008**, *31* (5), 1323–1333.
6. Massey, K. C.; Silton, S. I. Combining Experimental Data, Computational Fluid Dynamics, and Six-Degree of Freedom Simulation to Develop a Guidance Actuator for a Supersonic Projectile. *Journal of Aerospace Engineering*, **2009**, *223*, 341–355.
7. Davis, B.; Malejko, G.; Dorhn, R.; Owens, S.; Harkins, T.; Bischer, G. Addressing the Challenges of a Thruster-Based Precision Guided Mortar Munition With the Use of Embedded Telemetry Instrumentation. *ITEA Journal* **2009**, *30*, 117–125.
8. Fresconi, F.; Cooper, G. R.; Celmins, I.; DeSpirito, J.; Costello, M. Flight Mechanics of a Novel Guided Spin-Stabilized Projectile Concept. *Journal of Aerospace Engineering* **2011**, *226*, 327–340.
9. Fresconi, F. E. Guidance and Control of a Projectile with Reduced Sensor and Actuator Requirements. *Journal of Guidance, Control, and Dynamics* **2011**, *34* (6), 1757–1766.
10. Cooper, G. R.; Fresconi, F. E.; Costello, M. F. Flight Stability of an Asymmetric Projectile with Activating Canards. *Journal of Spacecraft and Rockets* **2012**, *49* (1), 130–135.
11. Fresconi, F. E.; Harkins, T. Experimental Flight Characterization of Asymmetric and Maneuvering Projectiles from Elevated Gun Firings. *Journal of Spacecraft and Rockets* **2012**, *49* (6), 1120–1130.

12. Brown, T. G.; Davis, B.; Hepner, D.; Faust, J.; Myers, C.; Muller, P.; Harkins, T.; Hollis, M.; Miller, C.; Placzankis, B. Strap-down Microelectromechanical (MEMS) Sensors for High-G Munition Applications. *IEEE Transactions on Magnetics* **2001**, *37* (1), 336–342.

13. Carlucci, D. E.; Frydman, A. M.; Cordes., J. A. Mathematical Description of Projectile Shot Exit Dynamics (Set Forward). *Journal of Applied Mechanics* **2013**, *80*, 031501-1-9.

14. Guidos, B.G.; Celmins, I. *The 40-mm M433 Projectile Aerodynamics Obtained from Spark Range Firings;* ARL-TR-4619; U.S. Army Research Laboratory: Aberdeen Proving Ground, MD, October 2008.

15. Pillay, P.; Krishnan, R. Modeling, Simulation, and Analysis of Permanent-Magnet Motor Drives, Part II: The Brushless D.C. Motor Drive. *IEEE Transactions on Industry Applications* **1989**, *25* (2), 274–279.

16. Hemati, N.; Leu, M. A Complete Model Characterization of Brushless DC Motors. *IEEE Transactions on Industry Applications* **1992**, *28* (1), 172–180.

17. Rigatos, G.G. Particle and Kalman Filtering for State Estimation and Control of DC Motors. *ISA Transactions* **2009**, *48*, 62–72.

18. Chapman, G.; Kirk, D. A New Method for Extracting Aerodynamic Coefficients from Free-Flight Data. *AIAA Journal* **1970**, *8* (4), 753–758.

19. Whyte, R. H.; Mermagen, W. H. A Method for Obtaining Aerodynamic Coefficients from Yawsonde and Radar Data. *Journal of Spacecraft and Rockets* **1973**, *10* (6), 384–388.

20. Hathaway, W.; Whyte, R. *Aeroballistic Research Facility Free Flight Data Analysis Using the Maximum Likelihood Method*; AFATL-TR-79-98; Air Force Armament Laboratory: Eglin Air Force Base, FL, December 1979.

21. Iliff, K. Parameter Estimation for Flight Vehicles. *Journal of Guidance* **1989**, *12* (5), 609–622.

22. Klein, V.; Morelli, E. A. Aircraft System Identification, AIAA Education Series, Reston, VA, 2006.

NO. OF COPIES	ORGANIZATION
1 (PDF)	DEFENSE TECHNICAL INFORMATION CTR DTIC OCA
1 (PDF)	DIRECTOR US ARMY RESEARCH LAB IMAL HRA
1 (PDF)	DIRECTOR US ARMY RESEARCH LAB RDRL CIO LL
1 (PDF)	GOVT PRINTG OFC A MALHOTRA
2 (PDF)	ARO S STANTON B GLAZ
7 (PDF)	RDECOM AMRDEC L AUMAN J DOYLE S DUNBAR B GRANTHAM M MCDANIEL C ROSEMA R SCHMALBACH
1 (PDF)	RDECOM ECBC D WEBER
31 (PDF)	RDECOM ARDEC D CARLUCCI S K CHUNG D L CLER D DEMELLA M DUCA G FLEMING R FULLERTON R GORMAN J C GRAU M HOHIL M HOLLIS R HOOKE W KOENIG A LICHTENBERG-SCANLAN S LONGO E LOGSDON M LUCIANO P MAGNOTTI G MALEJKO G MINER J MURNANE M PALATHINGAL

NO. OF COPIES	ORGANIZATION
	D PANHORST A PIZZA T RECCHIA B SMITH C STOUT W TOLEDO E VAZQUEZ L VO C WILSON
4 (PDF)	PEO AMMO C GRASSANO P MANZ R KOWALSKI, T CORADESCHI
2 (PDF)	PM CAS P BURKE M BURKE
1 (PDF)	MCOE A WRIGHT
2 (PDF)	ONR P CONOLLY D SIMONS
2 (PDF)	NSWCDD L STEELMAN K PAMADI
1 (PDF)	AFOSR EOARD G ABATE
1 (PDF)	MARCORSYSCOM P FREEMYERS
2 (PDF)	DARPA J DUNN K MASSEY
1 (PDF)	DRAPER LAB G THOREN
1 (PDF)	GTRI A LOVAS
3 (PDF)	ISL C BERNER S THEODOULIS P WERNERT

NO. OF COPIES ORGANIZATION

1 (PDF) DRDC
D CORRIVEAU

2 (PDF) GEORGIA INST OF TECHLGY
M COSTELLO
J ROGERS

1 (PDF) ROSE HULMAN INST OF TECHLGY
B BURCHETT

1 (PDF) AEROPREDICTION INC
F MOORE

1 (PDF) ARROW TECH
W HATHAWAY

3 (PDF) ATK
R DOHRN
B BECKER
S OWENS

3 (PDF) BAE
B GOODELL
P JANKE
O QUORTRUP

1 (PDF) GD OTS
D EDMONDS

3 (PDF) UTAS
P FRANZ
S ROUEN
M WILSON

ABERDEEN PROVING GROUND

55 (PDF) DIR USARL
RDRL WM
P J BAKER
RDRL WML
P J PEREGINO
M J ZOLTOSKI
RDRL WML A
M ARTHUR
W F OBERLE III
R PEARSON
L STROHM
RDRL WML B
N J TRIVEDI
RDRL WML C
S A AUBERT
RDRL WML D
R A BEYER
A BRANT
J COLBURN
M NUSCA
Z WINGARD
RDRL WML E
V A BHAGWANDIN
I CELMINS
J DESPIRITO
L D FAIRFAX
F E FRESCONI III
J M GARNER
B J GUIDOS JR
K R HEAVEY
R M KEPPINGER
G S OBERLIN
T PUCKETT
J SAHU
S I SILTON
P WEINACHT
RDRL WML F
B ALLIK
G BROWN
E BUKOWSKI
B S DAVIS
M DON
M HAMAOUI
K HUBBARD
M ILG
B KLINE
J MALEY
C MILLER
P MULLER
B NELSON
B TOPPER
RDRL WML G
A ABRAHAMIAN
M BERMAN
M CHEN
W DRYSDALE
M MINNICINO
J T SOUTH
RDRL WML H
T EHLERS
M FERMEN-COKER
J F NEWILL
R PHILABAUM
R SUMMERS
RDRL WMM
J S ZABINSKI
RDRL WMP
D H LYON

2 (PDF) DSTL
T BIRCH
R CHAPLIN